

- er, H. Eds., Kluwer, Dordrecht, Netherlands, 1990. (c) *Scanning Tunneling Microscopy I, II, III*; Wiesendanger, R.; Guntherodt, H.-J. Eds.; Springer, Heidelberg, 1992-1993. (d) *Scanning Tunneling Microscopy: Theory and Application*; Bonnel, D. Ed.; VCH, New York, 1993.
6. Meuris, M.; Heyns, M. M.; Mertens, P. W.; Verhaverbeke, S.; Philipossian, A. *Microcontamination* 10-5, 1992, p 31.
  7. Heyns, M. M.; Verhaverbeke, S.; Meuris, M.; Mertens, P. W.; Schmidt, H.; Kubota, M.; Philipossian, A.; Dillenbeck, K.; Graf, D.; Schnegg, A.; De Blank, R. *Mat. Res. Soc. Symp. Proc.* 1993, 315, 15.
  8. Aoyama, T.; Yamazaki, T.; Ito, T. *J. Electrochem. Soc.* 1996, 143, 2280.
  9. Lee, C. H.; Yu, K. S.; Jung, D. *J. Kor. Phys. Soc.*, submitted.

## Effect of Li on the Ionic Conductivity and Leaching in Simulated Borosilicate Glasses

Jong-Gyu Lee, Jong Goo Kim, Seung Soo Kim, Kwang Yong Jee, and Kwan Sik Chun

KAERI, Yusung P.O. Box 105, Taejeon 305-600, Korea

Received March 11, 1997

The ionic conductivity of several simulated borosilicate glasses was measured in the temperature range 150-600 °C in air. Leaching experiments were also carried out using Soxhlet apparatus at 100 °C for 7 days. As Li<sup>+</sup> ion increased in simulated borosilicate glasses, both the ionic conductivity and leaching rate increased. The activation energy in the ionic conduction of the simulated borosilicate glasses was 1.38-1.45 eV in the high temperature region and 0.93-1.1 eV in the low temperature region.

### Introduction

Electrical conductivity is one of the most important properties of glass at low temperature, especially when the glass is used as an insulating material or as a component of electrochemical devices. The electrical conductivity of glasses increases with temperature according to the exponential relation  $\mu = \mu_0 \exp(-E/RT)$ , where E is an activation energy for the electrical conduction. Not only the electrical conductivity (here, ionic conductivity), but also the corrosion rate is proportional to the concentration and diffusion rate of charge carriers, mostly cations in case of glass.<sup>1</sup> Thus, an exponential relationship between phenomena  $S = \text{const} \exp(-E/RT)$  is sought, where S is the rate of attack by solvent or dissolution reaction rate and E is an activation energy, usually 15-19 kcal/mol.<sup>2</sup> In 1949, Israd and Douglas were able to obtain a quantitative correlation between the rate of removal of alkali by water attack and the electrical conductivity, where both processes involve the diffusion of sodium ions.<sup>3</sup> However, the results of Das and Douglas showed that the correlation does not exist for less durable glasses.<sup>4</sup>

Borosilicate glass has been considered as one of the best matrix materials to isolate the high-level radioactive waste safely, because of its excellent chemical durability, good capability to accommodate and immobilize various radionuclides, and simple vitrification procedure, etc.<sup>5</sup> In fact, a borosilicate glass such as SON68 has been produced in Marcoule in France to use in the vitrification process of high-level radioactive waste since 1978.<sup>5</sup> In U.S.A., it has also been selected as the reference waste form for tank

wastes stored at Savannah River, West Valley and Hanford.<sup>6</sup>

In this report, the change of ionic conductivity as well as the leaching rate of simulated waste borosilicate glasses with increasing Li<sup>+</sup> ion are discussed. The effect of incorporation of fission products into the borosilicate glass on ionic conductivity is also discussed.

### Experimental

**Synthesis.** Disc-shaped samples of several simulated borosilicate glasses were prepared by a molding method. The stoichiometric amounts of SiO<sub>2</sub> (Merck, TLC G-type 60), B<sub>2</sub>O<sub>3</sub> (Showa, C.P.), Li<sub>2</sub>CO<sub>3</sub> (Aldrich, 99.997%), Na<sub>2</sub>CO<sub>3</sub> (Junsei, E.P.), CaO (Fisher, ACS), Al<sub>2</sub>O<sub>3</sub> (Aldrich, 99.9%), ZnO (Hayashi, C.P.), ZrO<sub>2</sub> (Aldrich, 99.99%), P<sub>2</sub>O<sub>5</sub> (Chameleon, C.P.), Fe<sub>2</sub>O<sub>3</sub> (Johnson Matthey, Spectro.), NiO (Junsei, C.P.), Cr<sub>2</sub>O<sub>3</sub> (Showa, E.P.), TeO<sub>2</sub> (Aldrich, 99.995%), Cs<sub>2</sub>O (Aldrich, 99% <), SrO (Aldrich, 99.995%), MoO<sub>3</sub> (Yoneyama, E.P.), MnO<sub>2</sub> (Junsei, C.P.), CoO (Junsei, C.P.), BaCO<sub>3</sub> (Aldrich, ACS), La<sub>2</sub>O<sub>3</sub> (Wako, 99% <), CeO<sub>2</sub> (Aldrich, 99.999%), Nd<sub>2</sub>O<sub>3</sub> (Cerac, 99.9%), Pr<sub>6</sub>O<sub>11</sub> (Aldrich, 99.999%), CdO (Junsei, C.P.), SnO<sub>2</sub> (Aldrich, 99.999%), Sb<sub>2</sub>O<sub>3</sub> (Shinyo, G.R.), Y<sub>2</sub>O<sub>3</sub> (Aldrich, 99.999%), and Ag<sub>2</sub>O (Kojima, 99% <) were mixed in glove box and heated in alumina crucible at 1200 °C for 2 hours (Table 1). A sample rod was made by pouring the molten glass into a preheated bright-red cylindrical mold with 12 mm diameter. The mold was made of stainless steel or Monel. It was then annealed at 500 °C for 1 hour and slowly cooled to room temperature by turning off the furnace. The cooled glass rod was cut by 1.2-1.6 mm thickness with diamond

**Table 1.** Composition of starting materials and products for the simulated borosilicate and normal borosilicate glasses

Composition	SW <sup>a</sup> (%)	SWFP2		SWFP5		SWFP10	
		Reactant (%)	Product (%)	Reactant (%)	Product (%)	Reactant (%)	Product (%)
SiO <sub>2</sub>	54.2	45.87	43.5	44.46	-	42.09	-
B <sub>2</sub> O <sub>3</sub>	16.7	14.14	12.7	13.71	13.2	12.98	12.1
Li <sub>2</sub> CO <sub>3</sub>	2.4	2.00	2.3	5.00	5.5	10.06	10.5
Na <sub>2</sub> CO <sub>3</sub>	11.8	9.95	10.5	9.64	9.5	9.12	9.0
CaO	4.8	4.08	5.6	3.95	5.4	3.74	5.1
Al <sub>2</sub> O <sub>3</sub> <sup>b</sup>	5.9	4.95	9.6	4.80	9.5	4.54	11.3
ZnO	3.0	2.52	2.3	2.44	2.4	2.31	2.2
ZrO <sub>2</sub>	1.2	2.67	1.9	2.58	1.5	2.45	2.1
P <sub>2</sub> O <sub>5</sub>		0.28	-	0.27	-	0.26	-
C.P. <sup>c</sup>		4.20	-	4.07	-	3.85	-
F.P. <sup>d</sup>		9.34	-	9.08	-	8.60	-
Total	100.0%	100.00%		100.00%		100.00%	

<sup>a</sup> Composition of SW borosilicate glass was obtained from the Cogema Incorp., Marcoule, France. <sup>b</sup> The increase of Al content in the products is due to the contamination from the alumina crucible during vitrification process. <sup>c</sup> C.P.: corrosion products such as Fe<sub>2</sub>O<sub>3</sub>, NiO, Cr<sub>2</sub>O<sub>3</sub>. <sup>d</sup> F.P.: fission products such as TeO<sub>2</sub>, Cs<sub>2</sub>O, SrO, MoO<sub>3</sub>, MnO<sub>2</sub>, CoO, BaCO<sub>3</sub>, La<sub>2</sub>O<sub>3</sub>, Ce<sub>2</sub>O<sub>3</sub>, Nd<sub>2</sub>O<sub>3</sub>, Pr<sub>2</sub>O<sub>3</sub>, CdO, SnO<sub>2</sub>, Sb<sub>2</sub>O<sub>3</sub>, Y<sub>2</sub>O<sub>3</sub> and Ag<sub>2</sub>CO<sub>3</sub>.

wheel blade. The surface of the glass discs was abraded with a 1200 grit SiC sandpaper. The disc samples were washed with alcohol before the ionic conductivity measurement and leaching experiment. Powdered samples of simulated borosilicate glasses were prepared by crushing and grinding the molten glass in an agate mortar and a pestle.

**Characterization.** Thermogravimetric (TGA) measurements were performed with a thermal analysis system (SETARAM TG-DTA92, France). The temperature was increased to 1200 °C by 30 °C/min, held for 2 hours and slowly cooled to room temperature by 10 °C/min. Composition of the simulated borosilicate glasses were analyzed by Electron probe microanalyzer (EPMA, JEOL JXA-8600) and by inductively coupled plasma emission (ICP, Jobin-Yvon JY 50P) and atomic absorption (AA, Perkin-Elmer 3100) spectrometers. For the ICP and AA analyses, the glass sample powder (approximately 0.1-0.12 g) was treated in the microwave sample digestion system (MLS-1200), using an acid mixture of 3 mL conc. HCl and 3 mL conc. HNO<sub>3</sub> (1 : 1). A part of the sample was remained unresolved, which seems to be due to silica. The soluble part of the sample was analyzed by ICP for B, Zn, Al, Ca and Zr and by AA for Li and Na. From the results of ICP and AA analyses, we confirmed the amounts of Li and B in the product are almost same with the charged values. The insoluble residue was treated using Li<sub>2</sub>B<sub>4</sub>O<sub>7</sub> flux for the analysis of unresolved part. Again there was a part of insoluble in the sample. The insoluble was weighed and assumed as SiO<sub>2</sub>. The additional soluble was analyzed by ICP and its amount was counted to the final composition.

**Leaching experiment.** The disc samples were tied with stainless steel wire and let dangled in the Soxhlet apparatus, which was made of Pyrex glass.<sup>7</sup> 125 mL of deionized water was added to the flask. The temperature of the heating mantle was increased slowly and refluxed at 100 °C for 7 days. After finishing leaching process, the solutions were diluted up to 150 mL with deionized water and analyzed by ICP. The leaching rate was corrected over the surface

area of the sample discs.

**AC impedance measurements.** AC impedance of the glasses was collected using two probe method with an impedance measurement system (IM5d, Zahner Elektrik, Germany). Contacts were made by painting both sides of sample disc with a silver paste. A sample holder was specially designed as shown in Figure 1. The holder was placed inside the quartz tube in a tube furnace, where the sample and electrodes were positioned in the hot zone of the furnace. In order to minimize the electromagnetic noise from the heating wire, the stainless steel sieve was inserted between the quartz tube and the Nichrome heating wire, and grounded well. Measurements were made in the temperature range 150-600 °C in air.

## Results and Discussion

As a result of composition analysis of major elements by ICP and AA (Table 1), most of the compositions of the major elements in simulated borosilicate glasses were found to be unchanged, except Al. Al content almost doubled due to a contamination from the alumina crucible during vitrification process. It was difficult to accurately determine

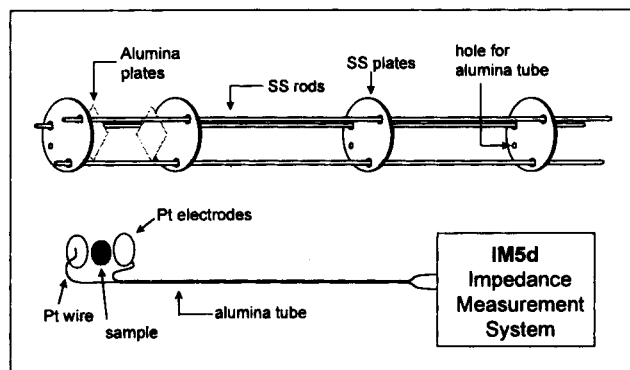


**Figure 1.** Schematic diagram of AC impedance measurement.

**Table 2.** Comparison of relative leaching of several simulated borosilicate glasses in Soxhlet apparatus for 1 week<sup>a</sup>

Glass	B	Na	Li	Si <sup>b</sup>	Al
SWFP2	3.32	3.83	1.47	7.67	1.18
SWFP5	3.83	5.08	2.80	7.87	1.46
SWFP10	8.51	15.5	7.55	13.9	14.4

<sup>a</sup>The values shown in this table is calculated from the equation, Relative elemental leaching rate=grams in solution/surface area of sample ( $\mu\text{g}/\text{cm}^2$ ). <sup>b</sup>The correction for the Si element as a background due to the leaching from the Soxhlet apparatus was not carried out.

the percentage of all the elements because of its small quantity in simulated borosilicate glass. A substantial amount of weight loss, ~28% was observed from TGA, which was accompanied with the decomposition of carbonates of starting materials. However, once the glass is formed, the weight loss of simulated borosilicate glass becomes much less 5-8%, which occurred mostly at high temperature 1200 °C.

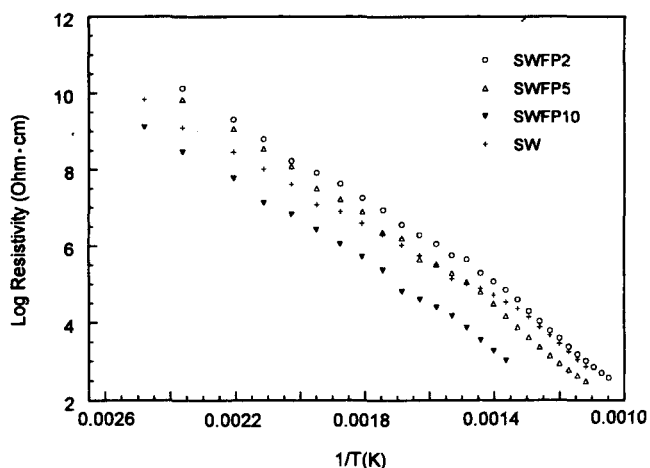
The results of leaching of simulated borosilicate glasses using Soxhlet apparatus for 1 week are listed in Table 2. The simulated borosilicate glasses containing 2-5%  $\text{Li}_2\text{O}$  showed very good leaching resistance. As Li content increased in simulated borosilicate glasses, SWFP2, SWFP5, SWFP10, leaching rate of each element increased. For Li<sup>+</sup> ion, leaching amount increased from 1.47 to 2.80-7.55, which is well consistent with the results of ionic conductivity measurements. For the other elements, B, Na, Si and Al, the leaching rate increased slightly when Li content increased from 2 to 5%. On the other hand, it increased greatly when Li content increased from 5 to 10%. This suggests that the Li content up to ~5% in simulated borosilicate glass does not produce so much loosely bound Li<sup>+</sup> ion any more which are formed most probably due to the fragmentation of three dimensional network.

The results of ionic conductivity measurements of simulated borosilicate glasses are shown in Table 3 and Figure 2. As Li<sup>+</sup> and Na<sup>+</sup> ion content increased, the resistivity decreased in the whole temperature range 150-600 °C. The resistivity data in Arrhenius plot (Figure 2) can be fit into two straight lines with different slopes, where both high temperature and low temperature regions are divided by

**Table 3.** Results of ac impedance measurements of several simulated and normal borosilicate glasses with typical fission products. The measurements are carried out in air in the temperature range 150-600 °C

Glass	Resistivity ( $\Omega \cdot \text{cm}$ )		$E_a$ (eV) <sup>a</sup>	$E_a$ (eV) <sup>b</sup>
	150 °C	460 °C		
SW	1.28 G	34.6 K	0.93	1.45
SWFP2	13.6 G	71.6 K	1.0	1.45
SWFP5	6.93 G	15.1 K	1.1	1.42
SWFP10	294 M	1.06 K	1.0	1.38

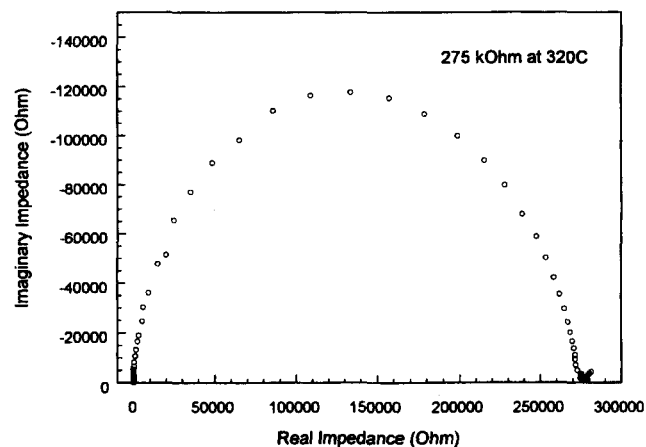
<sup>a</sup>Activation energy in low temperature region, 500-620 °C, 420-620 °C, 392-620 °C, 368-620 °C for SW, SWFP2, SWFP5, SWFP10, respectively. <sup>b</sup>Activation energy in high temperature region, 150-480 °C, 150-410 °C, 150-388 °C, 130-360 °C, for SW, SWFP2, SWFP5, SWFP10, respectively.

**Figure 2.** Arrhenius plots of several simulated borosilicate glasses.

transition temperature. The transition temperature was decreased from 413 to 391 and 365 °C as Li content increased from 2 to 5 and 10%. This means that the chains of three dimensional network structure built by network formers (Si, B) were discontinued by the incorporation of a large amount of Li<sup>+</sup> ion. Thus, the local structural units become smaller as Li content increases. In the high temperature region, the activation energy was slowly decreased from 1.45 to 1.42-1.38 eV, as Li content increases from 2 to 5-10%. However, in the low temperature region, the activation energy was not changed much, but remained at 0.93-1.1 eV. The charge carriers in these simulated borosilicate glasses are Li<sup>+</sup> and Na<sup>+</sup>. But Li<sup>+</sup> ion has much higher mobility and is expected to govern the ionic conductivity. Typical Nyquist diagram of the simulated borosilicate glass or normal borosilicate glass is depicted in Figure 3. It shows almost ideal semi-circle pattern.

## Conclusion

The simulated borosilicate glasses containing 2-5%  $\text{Li}_2\text{O}$  revealed good leaching resistance. As Li<sup>+</sup> ion increased in simulated borosilicate glasses, both the ionic conductivity and the leaching rate increased. The activation energy in the

**Figure 3.** Typical Nyquist plot of simulated borosilicate glass.

ionic conduction of the simulated borosilicate glasses was 1.38-1.45 eV in the high temperature region (500-620 °C, 420-620 °C, 392-620 °C, 368-620 °C for SW, SWFP2, SWFP5, SWFP10, respectively) and 0.93-1.1 eV in the low temperature region (150-480 °C, 150-410 °C, 150-388 °C, 130-360 °C, for SW, SWFP2, SWFP5, SWFP10, respectively).

### References

1. West, H. R. *Solid State Chemistry and its Applications*; John Wiley & Sons: New York, U. S. A., 1984; p 452.
2. White, W. B. In *Corrosion of Glass, Ceramic and Ceramic Superconductor*; Clark, D. E.; Zoitos, B. K., Ed.; Noyes Publ.: Park Ridge, New Jersey, U. S. A., 1992; p 21.
3. Douglas, R. W.; Israd, J. O. *J. Soc. Glass Technol.* **1949**, 33, 289.
4. Rawson, H. *Properties and Applications of Glass*; Elsevier: Netherlands, 1980; p 247.
5. Cunnane, J. C.; Bates, J. K.; Ebert, W. L.; Feng, X.; Mazer, J. J.; Wronkiewicz, D. J.; Sproull, J.; Boucier, W. L.; McGrail, B. P. *Mat. Res. Soc. Symp. Proc.* **1993**, 294, 225.
6. US Department of Energy Report, *Defense Waste Processing Facility: Savannah River Plant, Aiken, SC. Final environmental impact statement*, DOE/EIS-0082, 1982.
7. Nogues, J. L.; Vernaz, E. Y.; Jacquet-Francillon, N. *Mat. Res. Soc. Symp. Proc.* **1985**, 44, 89.

## Local Structure Refinement of the $\text{BaFe}_{1-x}\text{Sn}_x\text{O}_{3-y}$ System with Fe K-Edge X-Ray Absorption (XANES/EXAFS) Spectroscopy

Min Gyu Kim, Ki Seop Kwack, Kwon Sun Roh, and Chul Hyun Yo\*

Department of Chemistry, Yonsei University, Seoul 120-749, Korea  
Received April 7, 1997

Local structure refinement of the  $\text{BaFe}_{1-x}\text{Sn}_x\text{O}_{3-y}$  system ( $x=0.00-0.50$ ) has been carried out with Fe K-edge x-ray absorption spectroscopic studies. It is found out that the Fe ions are placed in two different symmetric sites such as tetrahedral and octahedral sites in the compounds by comparison with Fe K-edge x-ray absorption near edge structure (XANES) spectrum of the  $\gamma\text{-Fe}_2\text{O}_3$  compound as a reference. Small absorption peaks of dipole-forbidden transitions appear at a pre-edge region of 7111 eV due to the existence of Fe ions in the tetrahedral and octahedral sites. The peak intensity decreases with the substitution amount of Sn ion. Three different absorption peaks of  $1s \rightarrow 4p$  dipole-allowed transition appear on the energy region between 7123 and 7131 eV. The peaks correspond to  $1s \rightarrow 4p$  main transition of Fe ions in tetrahedral and octahedral sites and  $1s \rightarrow 4p$  transition followed by the shakedown process of ligand to metal charge transfer. The bond distances between Fe ions in the tetrahedral site and nearest neighboring oxygen atom (Fe-4O), and those in octahedral site (Fe-6O) are determined with the extended x-ray absorption fine structure (EXAFS) analysis. Two different interatomic distances increase with the substitution amount of Sn ion and also the bond lengths of Fe-4O are shorter than those of Fe-6O in all compounds.

### Introduction

The physical properties of perovskite-related metal oxides have been related closely to their structures. A number of studies for the transition metal oxides have been carried out extensively with various analytical methods in order to find relationships between their structures and physical properties. In general, physical properties such as electrical conductivity and magnetic susceptibility depend on the bonding character between transition metal and oxygen ions as well as the degree of local structural distortion on the transition metal elements.<sup>1-5</sup> Accurate structural refinement of compounds is important for the characterization of metal oxides.

Generally, oxygen nonstoichiometric perovskite-type oxides include both tetrahedral and octahedral sites for an atom. Therefore, it is difficult to determine the distance between each atomic site and ligand atom to molecular di-

mension scale with XRD since the atomic sites distribute randomly in the compounds. However, X-ray absorption spectroscopy is useful for structural analysis of the nonstoichiometric compounds since it is very specific to atomic local sites

Structural analysis of X-ray absorption (XANES/EXAFS) spectroscopy is used for local structure refinement on an interesting ion. For XANES (x-ray absorption near edge structure) spectroscopy, the spectra can result from the transition of a core electron to bound states. Therefore x-ray absorption pre-edge features give useful informations such as the oxidation state of chemical species, site symmetry of x-ray absorbing atom, and covalency. The dipole selection rules ( $\Delta l = \pm 1$ ) can be applied to the x-ray absorption spectroscopy, and the x-ray absorption occurs under an electron transition approximation. The dipole matrix element between an initial core state  $|i\rangle$  and a final state  $|f\rangle$  is fol-